Available online at www.sciencedirect.com

ScienceDirect

International Journal of Solids and Structures 45 (2008) 3153–3172

INTERNATIONAL JOURNAL OF SOLIDS AND STRUCTURES

www.elsevier.com/locate/ijsolstr

Finite deformation higher-order shell models and rigid-body motions

G.M. Kulikov [a,*], E. Carrera [b]

[a] *Department of Applied Mathematics and Mechanics, Tambov State Technical University, Sovetskaya Street 106, 392000 Tambov, Russia*
[b] *Department of Aeronautics and Aerospace Engineering, Politecnico di Torino, Corso Duca degli Abruzzi 24, 10129 Torino, Italy*

Received 17 September 2007; received in revised form 13 December 2007
Available online 31 January 2008

Abstract

This paper focuses on the developments of higher-order shell models by employing the new concept of *interpolation surfaces* (*I*-surfaces) inside the shell body. We introduce N ($N \geqslant 3$) *I*-surfaces and choose the values of displacements with correspondence to these surfaces as fundamental shell unknowns. Such choice allows, first, to develop various higher-order shell models in a very compact form and, second, to derive non-linear strain–displacement relationships, which are completely free for arbitrarily large rigid-body motions. The general $3N$-parameter shell model is proposed in the framework of the Lagrangian description. The special 9, 12 and 15 parameters cases (corresponding to $N = 3$, 4 and 5) have been dealt in detail. The proposed shell models account for thickness stretching and the complete 3D constitutive equations are utilized. The displacement vectors of equally located *I*-surfaces for each model are represented in a *convected* curvilinear coordinate system allowing one to develop directly finite deformation geometrically exact shell finite elements which could be discussed in future works.

Keywords: Finite deformation; Higher-order shell theory; Rigid-body motion; Interpolation surfaces; Lagrange polynomials

1. Introduction

One of the main requirements of any shell theory that is intended for application to computational mechanics (e.g. a finite element method) is that it must lead to strain-free modes for arbitrary rigid-body motions. The adequate representation of rigid-body motions is a necessary condition if good both accuracy and convergence properties are required. Therefore, when an inconsistent shell theory is utilized to develop any finite element, erroneous straining modes under rigid-body motions can be appeared. This problem has been studied for the classical Kirchhoff–Love shell theory by Cantin (1968) and Dawe (1972). Further developments for the finite deformation 6-parameter homogeneous and layer-wise shell theories based on the Mindlin kinematics have been done by Kulikov (2004) and Kulikov and Plotnikova (2003, 2006a). This work proposes higher-order

* Corresponding author. Fax: +7 475 263 0216.
E-mail addresses: kulikov@apmath.tstu.ru (G.M. Kulikov), erasmo.carrera@polito.it (E. Carrera).

0020-7683/$ - see front matter © 2008 Elsevier Ltd. All rights reserved.
doi:10.1016/j.ijsolstr.2008.01.020

shell theories on the basis of the strain–displacement equations, which exactly represent arbitrarily large rigid-body motions in a *convected* curvilinear coordinate system.

A large number of works has been already done to develop the finite deformation higher-order shell formulation (Librescu, 1987; Parisch, 1995; Sansour, 1995; Basar et al., 2000; El-Abbasi and Meguid, 2000; Sansour and Kollmann, 2000; Brank et al., 2002; Krätzig and Jun, 2003; Brank, 2005; Arciniega and Reddy, 2007) with thickness stretching. These articles except for purely theoretical contributions of Librescu (1987) and Krätzig and Jun (2003) are devoted to the 7-parameter shell theory in which the transverse normal strain varies at least linearly through the shell thickness. This fact is of great importance since the 6-parameter shell formulation based on the complete 3D constitutive equations exhibits thickness locking as mentioned in works (Kim and Lee, 1988; Buchter et al., 1994; Park et al., 1995; Kulikov, 2001; Sze, 2002; Kulikov and Plotnikova, 2006a; Carrera and Brischetto, 2007). The errors caused by thickness locking do not decrease with the mesh refinement because the reason of stiffening lies in the shell theory itself rather than the finite element discretization. We refer to review papers of Carrera (2002, 2003), where one may read that a conventional way for developing the higher-order shell formulation is to utilize either quadratic or cubic series expansions in the thickness coordinate and to choose as unknowns the generalized displacements of the reference (middle) surface. A Unified Formulation is also discussed in the latter paper (Carrera, 2003), which permits to develop plate/shell theories in terms of a few fundamental nuclei whose forms do not depend on the order of the used expansion.

In this paper, the higher-order shell models are developed by using the new concept that employs N *interpolation surfaces* (I-surfaces) inside the shell body, in order to choose displacements of these surfaces as fundamental unknowns. Such choice of displacements with the consequent use of the Lagrange polynomials in the thickness direction allows one to represent all three higher-order shell formulations developed in a compact form (similar to that used by Carrera, 2003) and to derive non-linear strain–displacement equations which are completely free for large rigid-body motions. Taking into account that displacement vectors of I-surfaces are introduced and resolved in the reference surface frame the proposed higher-order shell formulations are very promising for developing high performance finite rotation geometrically exact shell elements (Kulikov and Plotnikova, 2006b, 2007). The term "geometrically exact" reflects the fact that coefficients of the first and second fundamental forms, and Christoffel symbols are taken exactly at every Gauss integration point. Therefore, no approximation of the reference surface is needed. The advantage of the geometrically exact shell element formulation for coarse meshes is discussed in aforecited papers.

It should be mentioned that in some works (see e.g. Parisch, 1995; Kulikov, 2001, 2004; Carrera, 2003; Kulikov and Plotnikova, 2003, 2007) on solid-shell elements the displacement vectors of the bottom and top surfaces are also utilized. An idea of this approach can be traced back to the contribution of Schoop (1986). But in our higher-order shell formulation the use of bottom and top surfaces has a principally another mechanical sense: these are just a part of a set of I-surfaces inside the shell body. To substantiate this point of view, we remark that respectively $N = 3$, 4 and 5 equally located surfaces have been chosen as I-surfaces (such assumption is not mandatory, the I-surfaces could be also located with different relative distances). Thus, the resulting shell models are characterized by $3N$ parameters, i.e., we deal with 9, 12 and 15-parameter shell models.

It is of interest to notice that there is a connection between the proposed higher-order solid-shell model and the Lagrange continuum-based element (Zienkievicz and Taylor, 2000). The main difference consists in the fact that in our solid-shell formulation the Lagrange polynomials in the thickness direction are utilized before starting the discretization procedure by the finite element method. Thus, we deal with the stress resultant solid-shell theory, which permits one to derive equilibrium equations in both weak and strong forms. The latter can be useful for the analytical developments. Besides, the proposed solid-shell formulation based on the I-surface technique clears the way for developing efficient geometrically exact higher-order shell elements.

The attention of the present work has been restricted to the full description of fundamentals of the non-linear shell theory based on the I-surfaces including a weak form of equilibrium equations. The finite element formulations and their applications to homogeneous structures as well as the extension to laminated composite structures could be conveniently discussed in future developments.

2. Preliminaries

Let us consider a thick shell of the thickness h. The shell can be defined as a 3D body of volume V bounded by two outer surfaces Ω_b and Ω_t, located at the distances d_b and d_t measured with respect to the reference surface Ω, and the edge boundary surface Σ. The reference surface is assumed to be sufficiently smooth and without any singularities. Let the reference surface be referred to the general curvilinear coordinates θ^1 and θ^2, whereas the coordinate $\theta^3 = z$ is oriented along the unit vector $\boldsymbol{a}_3 = \boldsymbol{a}^3$ normal to the reference surface.

We now introduce all needed notations for describing the initial shell configuration (see Figs. 1 and 2):

– position vector of any point of the reference surface $\mathbf{r} = \mathbf{r}(\theta^1, \theta^2)$;
– covariant and contravariant base vectors of the reference surface

$$\boldsymbol{a}_\alpha = \mathbf{r}_{,\alpha}, \quad \boldsymbol{a}_\alpha \cdot \boldsymbol{a}^\beta = \delta_\alpha^\beta; \tag{1}$$

– covariant and contravariant components of the metric tensor of the reference surface

$$a_{\alpha\beta} = \boldsymbol{a}_\alpha \cdot \boldsymbol{a}_\beta, \quad a^{\alpha\beta} = \boldsymbol{a}^\alpha \cdot \boldsymbol{a}^\beta; \tag{2}$$

– determinant of the metric tensor of the reference surface $a = \det(a_{\alpha\beta})$;
– mixed components of the curvature tensor

$$b_\alpha^\beta = -\boldsymbol{a}^\beta \cdot \boldsymbol{a}_{3,\alpha}; \tag{3}$$

– position vector of any point in the shell body

$$\mathbf{R} = \mathbf{r} + \theta^3 \boldsymbol{a}_3; \tag{4}$$

– mixed components of the 3D shifter tensor

$$\mu_\alpha^\beta = \delta_\alpha^\beta - \theta^3 b_\alpha^\beta; \tag{5}$$

– covariant base vectors in the shell body

$$\mathbf{g}_\alpha = \mathbf{R}_{,\alpha} = \mu_\alpha^\beta \boldsymbol{a}_\beta, \quad \mathbf{g}_3 = \mathbf{R}_{,3} = \boldsymbol{a}_3; \tag{6}$$

– covariant components of the 3D metric tensor

$$g_{\alpha\beta} = \mathbf{g}_\alpha \cdot \mathbf{g}_\beta = \mu_\alpha^\gamma \mu_\beta^\delta a_{\gamma\delta}, \quad g_{i3} = \mathbf{g}_i \cdot \mathbf{g}_3 = \delta_{i3}; \tag{7}$$

– determinant of the 3D metric tensor $g = \det(g_{ij})$;
– determinant of the shifter tensor $\mu = \sqrt{g/a}$;

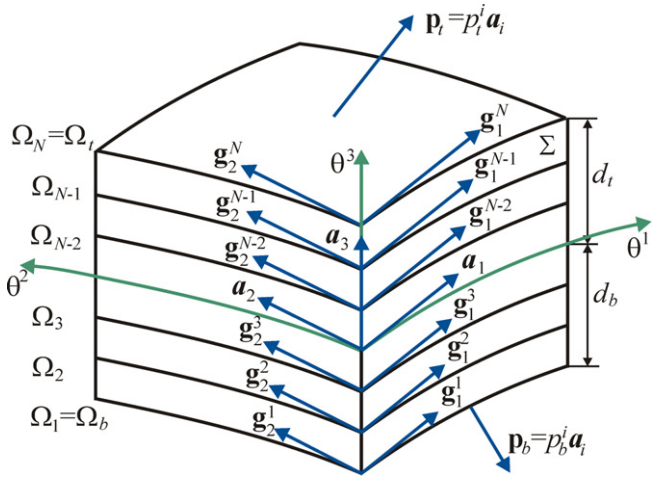

Fig. 1. Geometry of the shell and I-surfaces for the $3N$-parameter shell model.

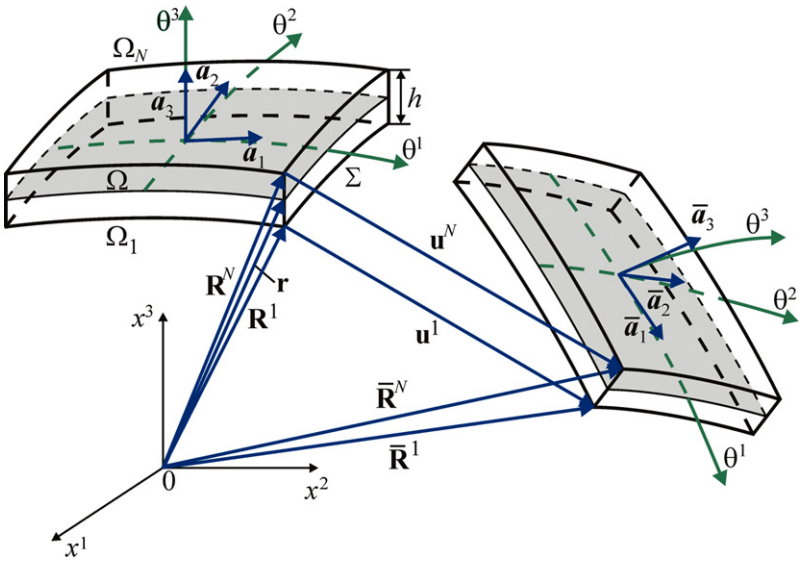

Fig. 2. Geometry and kinematics of the shell.

– I-surfaces $\Omega_1 = \Omega_b$, $\Omega_2, \ldots, \Omega_{N-1}$, $\Omega_N = \Omega_t$ defined by thickness coordinates

$$z_I = -d_b + (I-1)h/(N-1), \quad z_1 = -d_b, \quad z_N = d_t; \tag{8}$$

– position vectors of I-surfaces

$$\mathbf{R}^I = \mathbf{r} + z_I \boldsymbol{a}_3, \quad \mathbf{R}^1 = \mathbf{R}_b, \quad \mathbf{R}^N = \mathbf{R}_t; \tag{9}$$

– mixed components of the shifter tensors of I-surfaces

$$\mu_\alpha^{I\beta} = \delta_\alpha^\beta - z_I b_\alpha^\beta; \tag{10}$$

– covariant base vectors of I-surfaces

$$\mathbf{g}_\alpha^I = \mathbf{R}_{,\alpha}^I = \mu_\alpha^{I\beta} \boldsymbol{a}_\beta, \quad \mathbf{g}_3^I = \boldsymbol{a}_3; \tag{11}$$

– covariant components of the metric tensors of I-surfaces

$$g_{\alpha\beta}^I = \mathbf{g}_\alpha^I \cdot \mathbf{g}_\beta^I = \mu_\alpha^{I\gamma} \mu_\beta^{I\delta} a_{\gamma\delta}, \quad g_{i3}^I = \mathbf{g}_i^I \cdot \mathbf{g}_3^I = \delta_{i3}; \tag{12}$$

– determinants of the metric tensors of I-surfaces $g^I = \det(g_{ij}^I)$;
– determinants of the shifter tensors of I-surfaces $\mu^I = \sqrt{g^I/a}$;
– partial derivatives $(\ldots)_{,i}$ in V with respect to coordinates θ^i;
– covariant derivatives $(\ldots)|_\alpha$ in Ω with respect to coordinates θ^α.

Here and in the following developments, Greek tensorial indices α, β, γ, δ range from 1 to 2; Latin tensorial indices i, j, m, n range from 1 to 3; indices I, J, K identify the belonging of any quantity to the I-surfaces and run from 1 to N. Note also that from Eqs. (4), (6), (9) and (11) follow

$$\mathbf{R} = \frac{1}{h}(d_t - z)\mathbf{R}^1 + \frac{1}{h}(z + d_b)\mathbf{R}^N, \tag{13}$$

$$\mathbf{g}_\alpha = \frac{1}{h}(d_t - z)\mathbf{g}_\alpha^1 + \frac{1}{h}(z + d_b)\mathbf{g}_\alpha^N, \tag{14}$$

where base vectors of the bottom and top surfaces are

$$\mathbf{g}_\alpha^1 = \mu_\alpha^{1\beta} \boldsymbol{a}_\beta, \quad \mathbf{g}_\alpha^N = \mu_\alpha^{N\beta} \boldsymbol{a}_\beta. \tag{15}$$

2.1. 9-Parameter shell model

In accordance with Fig. 3(a) as I-surfaces the bottom, middle and top surfaces are chosen hence $N = 3$ and I runs from 1 to 3.

The position vector and base vectors of the shell can be expressed as

$$\mathbf{R} = L_I^3 \mathbf{R}^I, \tag{16}$$

$$\mathbf{g}_\alpha = L_I^3 \mathbf{g}_\alpha^I, \tag{17}$$

where $L_I^3(z)$ are the Lagrange polynomials of the second order defined as

$$\begin{aligned} L_1^3 &= \frac{2}{h^2}(z_2 - z)(z_3 - z), \\ L_2^3 &= \frac{4}{h^2}(z - z_1)(z_3 - z), \\ L_3^3 &= \frac{2}{h^2}(z - z_1)(z - z_2). \end{aligned} \tag{18}$$

Remark 1. From geometrical point of view we have

$$\mathbf{R}^1 = \mathbf{R}_b, \quad \mathbf{R}^2 = \frac{1}{2}\mathbf{R}_b + \frac{1}{2}\mathbf{R}_t, \quad \mathbf{R}^3 = \mathbf{R}_t. \tag{19}$$

The use of Eqs. (18) and (19) in Eq. (16) shows that both expressions for the position vector (13) and (16) are equivalent. The same conclusion can be done concerning base vectors (14) and (17).

2.2. 12-Parameter shell model

In this model, we choose four equally located I-surfaces as depicted in Fig. 3(b). Thus, $N = 4$ and I runs from 1 to 4.

The position vector and base vectors of the shell are written as

$$\mathbf{R} = L_I^4 \mathbf{R}^I, \tag{20}$$

$$\mathbf{g}_\alpha = L_I^4 \mathbf{g}_\alpha^I, \tag{21}$$

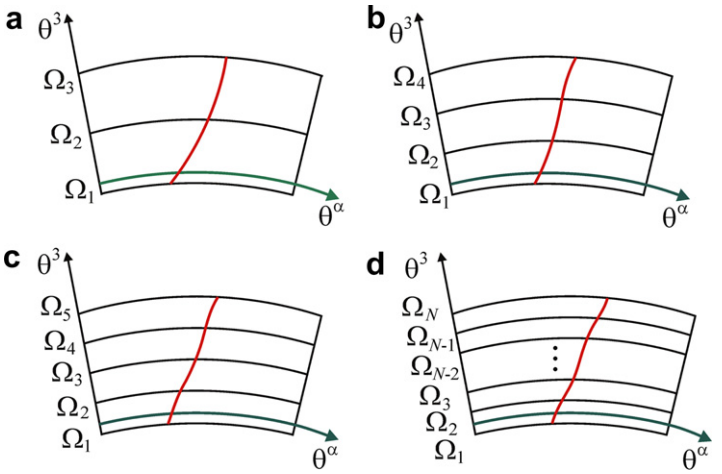

Fig. 3. Displacement field through the thickness of the shell for (a) 9-parameter model ($N = 3$), (b) 12-parameter model ($N = 4$), (c) 15-parameter model ($N = 5$), and (d) $3N$-parameter model.

where $L_I^4(z)$ are the Lagrange polynomials of the third order given by

$$\begin{aligned} L_1^4 &= \frac{9}{2h^3}(z_2 - z)(z_3 - z)(z_4 - z), \\ L_2^4 &= \frac{27}{2h^3}(z - z_1)(z_3 - z)(z_4 - z), \\ L_3^4 &= \frac{27}{2h^3}(z - z_1)(z - z_2)(z_4 - z), \\ L_4^4 &= \frac{9}{2h^3}(z - z_1)(z - z_2)(z - z_3). \end{aligned} \tag{22}$$

Remark 2. Using geometrical relations

$$\begin{aligned} &\mathbf{R}^1 = \mathbf{R}_b, \quad \mathbf{R}^2 = \frac{2}{3}\mathbf{R}_b + \frac{1}{3}\mathbf{R}_t, \\ &\mathbf{R}^3 = \frac{1}{3}\mathbf{R}_b + \frac{2}{3}\mathbf{R}_t, \quad \mathbf{R}^4 = \mathbf{R}_t \end{aligned} \tag{23}$$

and formulas for Lagrange polynomials (22) in Eqs. (20) and (21), we get again Eqs. (13) and (14).

2.3. 15-Parameter shell model

Herein, as displayed in Fig. 3(c), five equally located surfaces are chosen as *I*-surfaces, that is, $N = 5$ and I runs from 1 to 5.

The position vector and base vectors of the shell are written as

$$\mathbf{R} = L_I^5 \mathbf{R}^I, \tag{24}$$

$$\mathbf{g}_\alpha = L_I^5 \mathbf{g}_\alpha^I, \tag{25}$$

where $L_I^5(z)$ are the Lagrange polynomials of the fourth order defined as

$$\begin{aligned} L_1^5 &= \frac{32}{3h^4}(z_2 - z)(z_3 - z)(z_4 - z)(z_5 - z), \\ L_2^5 &= \frac{128}{3h^4}(z - z_1)(z_3 - z)(z_4 - z)(z_5 - z), \\ L_3^5 &= \frac{64}{h^4}(z - z_1)(z - z_2)(z_4 - z)(z_5 - z), \\ L_4^5 &= \frac{128}{3h^4}(z - z_1)(z - z_2)(z - z_3)(z_5 - z), \\ L_5^5 &= \frac{32}{3h^4}(z - z_1)(z - z_2)(z - z_3)(z - z_4). \end{aligned} \tag{26}$$

Remark 3. From geometrical point of view we have

$$\begin{aligned} &\mathbf{R}^1 = \mathbf{R}_b, \quad \mathbf{R}^2 = \frac{3}{4}\mathbf{R}_b + \frac{1}{4}\mathbf{R}_t, \quad \mathbf{R}^3 = \frac{1}{2}\mathbf{R}_b + \frac{1}{2}\mathbf{R}_t, \\ &\mathbf{R}^4 = \frac{1}{4}\mathbf{R}_b + \frac{3}{4}\mathbf{R}_t, \quad \mathbf{R}^5 = \mathbf{R}_t. \end{aligned} \tag{27}$$

As a result, corresponding Eqs. (13), (14), (24) and (25) are also equivalent.

2.4. 3N-parameter shell model

Finally, we choose N equally located I-surfaces as shown in Fig. 3(d). Therefore, the position vector and base vectors in the shell body can be represented as

$$\mathbf{R} = L_I^N \mathbf{R}^I, \tag{28}$$

$$\mathbf{g}_\alpha = L_I^N \mathbf{g}_\alpha^I, \tag{29}$$

where $L_I^N(z)$ are the Lagrange polynomials of the $(N-1)$th order and position vectors of I-surfaces are

$$\mathbf{R}^I = \frac{1}{h}(d_t - z_I)\mathbf{R}_b + \frac{1}{h}(d_b + z_I)\mathbf{R}_t.$$

This general shell formulation will not be considered in details anyway the developments in the next sections will conveniently refer to it.

3. Kinematic description of deformed shell

The *first fundamental assumption* for the proposed higher-order shell theory, which is partially illustrated in Fig. 3, is made at this point introduced.

Assumption 1. The displacement field is approximated in the thickness direction using general description of the $3N$-parameter shell model as follows:

$$\mathbf{u} = L_I^N \mathbf{u}^I, \tag{30}$$

where $\mathbf{u}^I(\theta^1, \theta^2)$ are the displacement vectors of I-surfaces.

From Eqs. (28) and (30) we find the following expression for the position vector of the deformed shell:

$$\overline{\mathbf{R}} = \mathbf{R} + \mathbf{u} = L_I^N \overline{\mathbf{R}}^I, \tag{31}$$

where $\overline{\mathbf{R}}^I(\theta^1, \theta^2)$ are the position vectors of I-surfaces given by

$$\overline{\mathbf{R}}^I = \mathbf{R}^I + \mathbf{u}^I. \tag{32}$$

Covariant base vectors in the current shell configuration, allowing for Eqs. (11) and (30)–(32), can be written as

$$\bar{\mathbf{g}}_\alpha = \overline{\mathbf{R}}_{,\alpha} = L_I^N \bar{\mathbf{g}}_\alpha^I, \tag{33a}$$

$$\bar{\mathbf{g}}_3 = \overline{\mathbf{R}}_{,3} = \boldsymbol{a}_3 + \boldsymbol{\beta}, \tag{33b}$$

where

$$\bar{\mathbf{g}}_\alpha^I = \overline{\mathbf{R}}_{,\alpha}^I = \mathbf{g}_\alpha^I + \mathbf{u}_{,\alpha}^I, \tag{34}$$

$$\boldsymbol{\beta} = \mathbf{u}_{,3} = L_{I,3}^N \mathbf{u}^I. \tag{35}$$

It is of extreme interest to notice that the introduction of the transverse rate vector $\boldsymbol{\beta}$ plays a central role in the present higher-order shell formulation. A discussion on that is made in section 5, where rigid-body motion representations of its vector at the I-surfaces are studied. The explicit forms of the derivatives of Lagrange polynomials $L_{I,3}^N$ for the three shell models are presented in Appendix A.

4. Strain–displacement relationships

According to the total Lagrangian description the energetically conjugate second Piola–Kirchhoff stress tensor and Green–Lagrange strain tensor are employed. The Green–Lagrange strain tensor can be written as

$$2\varepsilon_{ij} = \bar{\mathbf{g}}_i \cdot \bar{\mathbf{g}}_j - \mathbf{g}_i \cdot \mathbf{g}_j. \tag{36}$$

Substituting base vectors (33) into relationships (36) and allowing for Eqs. (29) and (34), one derives

$$2\varepsilon_{\alpha\beta} = L_I^N L_J^N (\mathbf{u}_{,\alpha}^I \cdot \mathbf{g}_\beta^J + \mathbf{u}_{,\beta}^J \cdot \mathbf{g}_\alpha^I + \mathbf{u}_{,\alpha}^I \cdot \mathbf{u}_{,\beta}^J), \tag{37a}$$

$$2\varepsilon_{\alpha 3} = L_I^N (\boldsymbol{\beta} \cdot \mathbf{g}_\alpha^I + \mathbf{u}_{,\alpha}^I \cdot \boldsymbol{a}_3 + \boldsymbol{\beta} \cdot \mathbf{u}_{,\alpha}^I), \tag{37b}$$

$$2\varepsilon_{33} = 2\boldsymbol{\beta} \cdot \boldsymbol{a}_3 + \boldsymbol{\beta} \cdot \boldsymbol{\beta}. \tag{37c}$$

The analysis of Eqs. (35) and (37) shows that: in-plane strains $\varepsilon_{\alpha\beta}$ are the polynomials of the $(2N-2)$th order; transverse shear strains $\varepsilon_{\alpha 3}$ are the polynomials of the $(2N-3)$th order; and a transverse normal strain ε_{33} is the polynomial of the $(2N-4)$th order.

To simplify the higher-order shell formulation, the *second fundamental assumption* of the present theory is introduced.

Assumption 2. All components of the Green–Lagrange strain tensor are distributed through the thickness of the shell according to the displacement distribution (30), that is,

$$\tilde{\varepsilon}_{ij} = L_I^N \varepsilon_{ij}^I, \tag{38}$$

where $\varepsilon_{ij}^I = \varepsilon_{ij}(z_I)$ are the *exact strains* of *I*-surfaces defined as

$$2\varepsilon_{\alpha\beta}^I = \mathbf{u}_{,\alpha}^I \cdot \mathbf{g}_\beta^I + \mathbf{u}_{,\beta}^I \cdot \mathbf{g}_\alpha^I + \mathbf{u}_{,\alpha}^I \cdot \mathbf{u}_{,\beta}^I, \tag{39a}$$

$$2\varepsilon_{\alpha 3}^I = \boldsymbol{\beta}^I \cdot \mathbf{g}_\alpha^I + \mathbf{u}_{,\alpha}^I \cdot \boldsymbol{a}_3 + \boldsymbol{\beta}^I \cdot \mathbf{u}_{,\alpha}^I, \tag{39b}$$

$$2\varepsilon_{33}^I = 2\boldsymbol{\beta}^I \cdot \boldsymbol{a}_3 + \boldsymbol{\beta}^I \cdot \boldsymbol{\beta}^I. \tag{39c}$$

Here, $\boldsymbol{\beta}^I(\theta^1, \theta^2)$ are the transverse rate vectors of *I*-surfaces given by

$$\boldsymbol{\beta}^I = \boldsymbol{\beta}(z_I) = L_{J,3}^N(z_I)\mathbf{u}^J. \tag{40}$$

As can be seen, this assumption is very robust because now all strain components $\tilde{\varepsilon}_{ij}$ are the polynomials of the $(N-1)$th order that simplifies sufficiently the higher-order shell formulation.

Remark 4. It can be verified using a property of Lagrange polynomials (18), (22) and (26), namely, $L_I^N(z_J) = \delta_{IJ}$ that simplified strains $\tilde{\varepsilon}_{ij}$ satisfy linking conditions

$$\tilde{\varepsilon}_{ij}(z_I) = \varepsilon_{ij}(z_I) = \varepsilon_{ij}^I.$$

This fact is illustrated in Fig. 4 by means of in-plane strains.

Let us represent displacement vectors of *I*-surfaces in a form

$$\mathbf{u}^I = u_i^I \boldsymbol{a}^i. \tag{41}$$

It should be remarked that displacement vectors are resolved in the contravariant reference surface basis $\boldsymbol{a}^i$ that allows us to reduce the computational cost of numerical integration in the evaluation of the stiffness matrix (Kulikov and Plotnikova, 2006b, 2007).

The derivatives from strain–displacement relationships (39) can be expressed as

$$\mathbf{u}_{,\alpha}^I = u_i^I|_\alpha \boldsymbol{a}^i, \tag{42}$$

$$u_i^I|_\alpha = u_{i,\alpha}^I - \Gamma_{i\alpha}^j u_j^I, \tag{43}$$

where $\Gamma_{i\alpha}^j$ are the Christoffel symbols defined as

$$\Gamma_\alpha^i\beta = \boldsymbol{a}^i \cdot \boldsymbol{a}_{\alpha,\beta}, \quad \Gamma_{3\alpha}^\beta = -b_\alpha^\beta, \quad \Gamma_{3\alpha}^3 = 0. \tag{44}$$

For the transverse rate vectors of *I*-surfaces we have the similar presentation in this contravariant basis

$$\boldsymbol{\beta}^I = \beta_i^I \boldsymbol{a}^i. \tag{45}$$

Substituting Eqs. (11), (42) and (45) into strain–displacement relationships (39), we can write these ones in a scalar form as

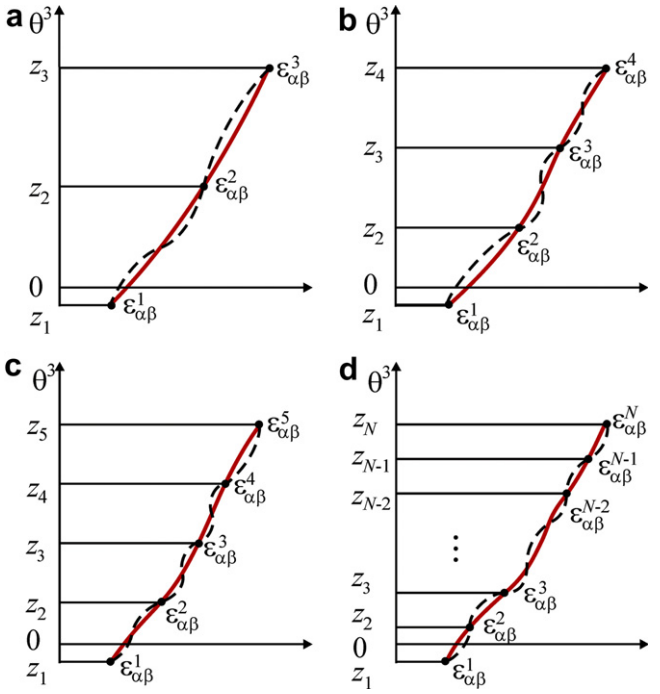

Fig. 4. Approximate $\tilde{\varepsilon}_{\alpha\beta}$ (——) and exact $\varepsilon_{\alpha\beta}$ (— —) in-plain strain distributions through the thickness of the shell for (a) 9-parameter model, where $\varepsilon_{\alpha\beta}$ and $\tilde{\varepsilon}_{\alpha\beta}$ are the polynomials of the fourth and second orders; (b) 12-parameter model, where $\varepsilon_{\alpha\beta}$ and $\tilde{\varepsilon}_{\alpha\beta}$ are the polynomials of the sixth and third orders; (c) 15-parameter model, where $\varepsilon_{\alpha\beta}$ and $\tilde{\varepsilon}_{\alpha\beta}$ are the polynomials of the eighth and fourth orders; and (d) $3N$-parameter model, where $\varepsilon_{\alpha\beta}$ and $\tilde{\varepsilon}_{\alpha\beta}$ are the polynomials of the $(2N-2)$th and $(N-1)$th orders.

$$2\varepsilon^I_{\alpha\beta} = \mu^{I\gamma}_{\beta} u^I_{\gamma}|_{\alpha} + \mu^{I\gamma}_{\alpha} u^I_{\gamma}|_{\beta} + a^{ij} u^I_i|_{\alpha} u^I_j|_{\beta}, \tag{46a}$$

$$2\varepsilon^I_{\alpha 3} = \mu^{I\gamma}_{\alpha} \beta^I_{\gamma} + u^I_3|_{\alpha} + a^{ij} \beta^I_i u^I_j|_{\alpha}, \tag{46b}$$

$$2\varepsilon^I_{33} = 2\beta^I_3 + a^{ij} \beta^I_i \beta^I_j. \tag{46c}$$

Here, for convenience it has been introduced an additional notation $a^{i3} = \delta^{i3}$. In orthogonal curvilinear reference surface coordinates the strain–displacement relationships (46) are represented in a simpler form and may be useful for the geometrically exact shell element formulation (Kulikov and Plotnikova, 2006b, 2007). This is discussed in Appendix B.

Finally, we consider presentations of the transverse rate vectors of I-surfaces for the developed shell models.

4.1. 9-Parameter shell model

In this model $N = 3$ and according to Eq. (40) we have

$$\boldsymbol{\beta}^I = L^3_{J,3}(z_I)\mathbf{u}^J. \tag{47}$$

The use of Eq. (47) and Table 1 leads to

$$\begin{aligned} \boldsymbol{\beta}^1 &= \frac{1}{h}(-3\mathbf{u}^1 + 4\mathbf{u}^2 - \mathbf{u}^3), \\ \boldsymbol{\beta}^2 &= \frac{1}{h}(-\mathbf{u}^1 + \mathbf{u}^3), \\ \boldsymbol{\beta}^3 &= \frac{1}{h}(\mathbf{u}^1 - 4\mathbf{u}^2 + 3\mathbf{u}^3). \end{aligned} \tag{48}$$

Table 1
Values of derivatives of Lagrange polynomials of the second order at I-surfaces

Coordinates	$L^3_{1,3}$	$L^3_{2,3}$	$L^3_{3,3}$
z_1	$-\frac{3}{h}$	$\frac{4}{h}$	$-\frac{1}{h}$
z_2	$-\frac{1}{h}$	0	$\frac{1}{h}$
z_3	$\frac{1}{h}$	$-\frac{4}{h}$	$\frac{3}{h}$

4.2. 12-Parameter shell model

In this model $N = 4$ and

$$\boldsymbol{\beta}^I = L^4_{J,3}(z_I)\mathbf{u}^J. \tag{49}$$

From Eq. (49) and Table 2 we derive

$$\begin{aligned}
\boldsymbol{\beta}^1 &= \frac{1}{2h}(-11\mathbf{u}^1 + 18\mathbf{u}^2 - 9\mathbf{u}^3 + 2\mathbf{u}^4),\\
\boldsymbol{\beta}^2 &= \frac{1}{2h}(-2\mathbf{u}^1 - 3\mathbf{u}^2 + 6\mathbf{u}^3 - \mathbf{u}^4),\\
\boldsymbol{\beta}^3 &= \frac{1}{2h}(\mathbf{u}^1 - 6\mathbf{u}^2 + 3\mathbf{u}^3 + 2\mathbf{u}^4),\\
\boldsymbol{\beta}^4 &= \frac{1}{2h}(-2\mathbf{u}^1 + 9\mathbf{u}^2 - 18\mathbf{u}^3 + 11\mathbf{u}^4).
\end{aligned} \tag{50}$$

4.3. 15-Parameter shell model

In this model $N = 5$ and

$$\boldsymbol{\beta}^I = L^5_{J,3}(z_I)\mathbf{u}^J. \tag{51}$$

Using Eq. (51) and Table 3, one finds

$$\begin{aligned}
\boldsymbol{\beta}^1 &= \frac{1}{3h}(-25\mathbf{u}^1 + 48\mathbf{u}^2 - 36\mathbf{u}^3 + 16\mathbf{u}^4 - 3\mathbf{u}^5),\\
\boldsymbol{\beta}^2 &= \frac{1}{3h}(-3\mathbf{u}^1 - 10\mathbf{u}^2 + 18\mathbf{u}^3 - 6\mathbf{u}^4 + \mathbf{u}^5),\\
\boldsymbol{\beta}^3 &= \frac{1}{3h}(\mathbf{u}^1 - 8\mathbf{u}^2 + 8\mathbf{u}^4 - \mathbf{u}^5),\\
\boldsymbol{\beta}^4 &= \frac{1}{3h}(-\mathbf{u}^1 + 6\mathbf{u}^2 - 18\mathbf{u}^3 + 10\mathbf{u}^4 + 3\mathbf{u}^5),\\
\boldsymbol{\beta}^5 &= \frac{1}{3h}(3\mathbf{u}^1 - 16\mathbf{u}^2 + 36\mathbf{u}^3 - 48\mathbf{u}^4 + 25\mathbf{u}^5).
\end{aligned} \tag{52}$$

Table 2
Values of derivatives of Lagrange polynomials of the third order at I-surfaces

Coordinates	$L^4_{1,3}$	$L^4_{2,3}$	$L^4_{3,3}$	$L^4_{4,3}$
z_1	$-\frac{11}{2h}$	$\frac{9}{h}$	$-\frac{9}{2h}$	$\frac{1}{h}$
z_2	$-\frac{1}{h}$	$-\frac{3}{2h}$	$\frac{3}{h}$	$-\frac{1}{2h}$
z_3	$\frac{1}{2h}$	$-\frac{3}{h}$	$\frac{3}{2h}$	$\frac{1}{h}$
z_4	$-\frac{1}{h}$	$\frac{9}{2h}$	$-\frac{9}{h}$	$\frac{11}{2h}$

Table 3
Values of derivatives of Lagrange polynomials of the fourth order at I-surfaces

Coordinates	$L^5_{1,3}$	$L^5_{2,3}$	$L^5_{3,3}$	$L^5_{4,3}$	$L^5_{5,3}$
z_1	$-\frac{25}{3h}$	$\frac{16}{h}$	$-\frac{12}{h}$	$\frac{16}{3h}$	$-\frac{1}{h}$
z_2	$-\frac{1}{h}$	$-\frac{10}{3h}$	$\frac{6}{h}$	$-\frac{2}{h}$	$\frac{1}{3h}$
z_3	$\frac{1}{3h}$	$-\frac{8}{3h}$	0	$\frac{8}{3h}$	$-\frac{1}{3h}$
z_4	$-\frac{1}{3h}$	$\frac{2}{h}$	$-\frac{6}{h}$	$\frac{10}{3h}$	$\frac{1}{h}$
z_5	$\frac{1}{h}$	$-\frac{16}{3h}$	$\frac{12}{h}$	$-\frac{16}{h}$	$\frac{25}{3h}$

4.4. 3N-parameter shell model

The extension to the case of N I-surfaces is for sake of brevity omitted. However, such an extension does not introduce any difficulties.

5. Rigid-body motions

An arbitrarily large rigid-body motion can be defined as

$$(\mathbf{u})^{\text{Rigid}} = \Delta + (\Phi - \mathbf{I})\mathbf{R}, \tag{53}$$

where $\Delta = \Delta_i \boldsymbol{a}^i$ is the constant displacement (translation) vector; $\mathbf{I}$ is the identity matrix; Φ is the orthogonal rotation matrix (see e.g. Kulikov, 2004). In particular, rigid-body displacements of I-surfaces are written as

$$(\mathbf{u}^I)^{\text{Rigid}} = \Delta + \Phi\mathbf{R}^I - \mathbf{R}^I \tag{54}$$

and derivatives of first two terms will be

$$\Delta_{,\alpha} = \mathbf{0}, \tag{55}$$

$$(\Phi\mathbf{R}^I)_{,\alpha} = \Phi\mathbf{R}^I_{,\alpha} = \Phi\mathbf{g}^I_\alpha. \tag{56}$$

Using Eqs. (54)–(56), one obtains

$$(\mathbf{u}^I_{,\alpha})^{\text{Rigid}} = \Phi\mathbf{g}^I_\alpha - \mathbf{g}^I_\alpha. \tag{57}$$

Substituting rigid-body displacements (54) into Eq. (48) and taking into account Eqs. (9) and (19), we derive

$$\begin{aligned}(\boldsymbol{\beta}^1)^{\text{Rigid}} &= \frac{1}{h}\{-3[\Delta + (\Phi - \mathbf{I})\mathbf{R}^1] + 4[\Delta + (\Phi - \mathbf{I})\mathbf{R}^2] - [\Delta + (\Phi - \mathbf{I})\mathbf{R}^3]\} \\ &= \frac{1}{h}(\Phi - \mathbf{I})(-3\mathbf{R}^1 + 4\mathbf{R}^2 - \mathbf{R}^3) = \frac{1}{h}(\Phi - \mathbf{I})(\mathbf{R}_t - \mathbf{R}_b) = \Phi\boldsymbol{a}_3 - \boldsymbol{a}_3,\end{aligned} \tag{58a}$$

$$\begin{aligned}(\boldsymbol{\beta}^2)^{\text{Rigid}} &= \frac{1}{h}\{-\Delta - (\Phi - \mathbf{I})\mathbf{R}^1 + \Delta + (\Phi - \mathbf{I})\mathbf{R}^3\} = \frac{1}{h}(\Phi - \mathbf{I})(\mathbf{R}^3 - \mathbf{R}^1) = \frac{1}{h}(\Phi - \mathbf{I})(\mathbf{R}_t - \mathbf{R}_b) \\ &= \Phi\boldsymbol{a}_3 - \boldsymbol{a}_3,\end{aligned} \tag{58b}$$

$$\begin{aligned}(\boldsymbol{\beta}^3)^{\text{Rigid}} &= \frac{1}{h}\{[\Delta + (\Phi - \mathbf{I})\mathbf{R}^1] - 4[\Delta + (\Phi - \mathbf{I})\mathbf{R}^2] + 3[\Delta + (\Phi - \mathbf{I})\mathbf{R}^3]\} \\ &= \frac{1}{h}(\Phi - \mathbf{I})(\mathbf{R}^1 - 4\mathbf{R}^2 + 3\mathbf{R}^3) = \frac{1}{h}(\Phi - \mathbf{I})(\mathbf{R}_t - \mathbf{R}_b) = \Phi\boldsymbol{a}_3 - \boldsymbol{a}_3.\end{aligned} \tag{58c}$$

In a general notation formulas (58) are written as

$$(\boldsymbol{\beta}^I)^{\text{Rigid}} = \Phi\boldsymbol{a}_3 - \boldsymbol{a}_3. \tag{59}$$

Note that these results can be easily extended to the 12-parameter and 15-parameter shell models employing correspondingly Eqs. (9), (23) and (50), and Eqs. (9), (27) and (52).

It may be verified by using Eqs. (57) and (59) that strains of I-surfaces (39) are all zero in a general large rigid-body motion:

$$2(\varepsilon_{ij}^{I})^{\text{Rigid}} = (\Phi \mathbf{g}_i^I) \cdot (\Phi \mathbf{g}_j^I) - \mathbf{g}_i^I \cdot \mathbf{g}_j^I = 0. \tag{60}$$

This conclusion is true because an orthogonal transformation retains the scalar product of vectors. So, due to relations (60) Green–Lagrange strains (38) exactly represent arbitrarily large rigid-body motions, that is,

$$(\tilde{\varepsilon}_{ij})^{\text{Rigid}} = L_I^N (\varepsilon_{ij}^I)^{\text{Rigid}} = 0. \tag{61}$$

The results obtained in this section clearly show the convenience of referring to I-surfaces in the development of higher-order theories for shells.

6. Principle of virtual work

The internal virtual work in a 3D shell body is expressed as

$$\delta W_{\text{int}} = \iiint_V \mu s^{ij} \delta \tilde{\varepsilon}_{ij} \sqrt{a}\, \mathrm{d}\theta^1\, \mathrm{d}\theta^2\, \mathrm{d}\theta^3, \tag{62}$$

where s^{ij} are the components of the second Piola–Kirchhoff stress tensor.

Substituting strains (38) in Eq. (62) and introducing stress resultants

$$S_I^{ij} = \int_{-d_b}^{d_t} \mu s^{ij} L_I^N \, \mathrm{d}\theta^3, \tag{63}$$

one finds

$$\delta W_{\text{int}} = \iint_\Omega S_I^{ij} \delta \varepsilon_{ij}^I \sqrt{a}\, \mathrm{d}\theta^1\, \mathrm{d}\theta^2. \tag{64}$$

This study focuses on linear elastic materials. The natural choice for constitutive equations is the generalized Hooke's law:

$$s^{ij} = C^{ijmn} \tilde{\varepsilon}_{mn}, \tag{65}$$

where C^{ijmn} are the components of the material tensor.

The use of Eqs. (38) and (65) in a formula for stress resultants (63) yields

$$S_I^{ij} = D_{IJ}^{ijmn} \varepsilon_{mn}^J, \tag{66}$$

where

$$D_{IJ}^{ijmn} = \int_{-d_b}^{d_t} \mu C^{ijmn} L_I^N L_J^N \, \mathrm{d}\theta^3. \tag{67}$$

Remark 5. To carry out the exact analytical integration[1] in Eq. (67), the determinant of the 3D shifter tensor can be approximated by applying the Lagrange expansion that has been extensively used in this paper, i.e.,

$$\mu = L_K^N \mu^K, \tag{68}$$

where values of this determinant at the I-surfaces are

$$\mu^K = \sqrt{g^K / a}. \tag{69}$$

As a result, the following compact and convenient formula is obtained:

[1] By using any software for the symbolic mathematical analysis.

$$D_{IJ}^{ijmn} = \int_{-d_b}^{d_t} \mu^K C^{ijmn} L_I^N L_J^N L_K^N \, \mathrm{d}\theta^3. \tag{70}$$

In practice, for thin shells the simplest approximation may be employed

$$\mu = \frac{1}{N} \sum_K \mu^K. \tag{71}$$

Consider next the virtual work of the external forces. For the sake of simplicity we limit our discussion to conservative surface loading. In such case one obtains

$$\delta W_{\mathrm{ext}} = \iint_\Omega (\mu^N p_t^i \delta u_i^N - \mu^1 p_b^i \delta u_i^1) \sqrt{a} \, \mathrm{d}\theta^1 \, \mathrm{d}\theta^2 + \delta W_{\mathrm{ext}}^\Sigma, \tag{72}$$

where $\delta W_{\mathrm{ext}}^\Sigma$ is the virtual work done by external loads acting on the boundary surface Σ; p_b^i and p_t^i are the contravariant components of the traction vectors $\mathbf{p}_b$ and $\mathbf{p}_t$ applied to the bottom and top surfaces.

The principle of the virtual work is now stated as

$$\delta W_{\mathrm{int}} = \delta W_{\mathrm{ext}}. \tag{73}$$

From the principal of the virtual work we can derive equilibrium equations in both weak and strong forms. However, the latter is usually not considered for computational developments. Thus, our attention will be restricted to the weak form formulation.

7. Weak form of equilibrium equations

It is well known that the use of the tensor-based shell formulation in conjunction with higher-order elements for the non-linear analysis of both thin and thick shells leads to an effective computational approach. In this context, we address concisely an implementation of the proposed 9-parameter shell formulation for constructing geometrically exact shell elements (Fig. 5). The term "geometrically exact" is explained in Section 1.

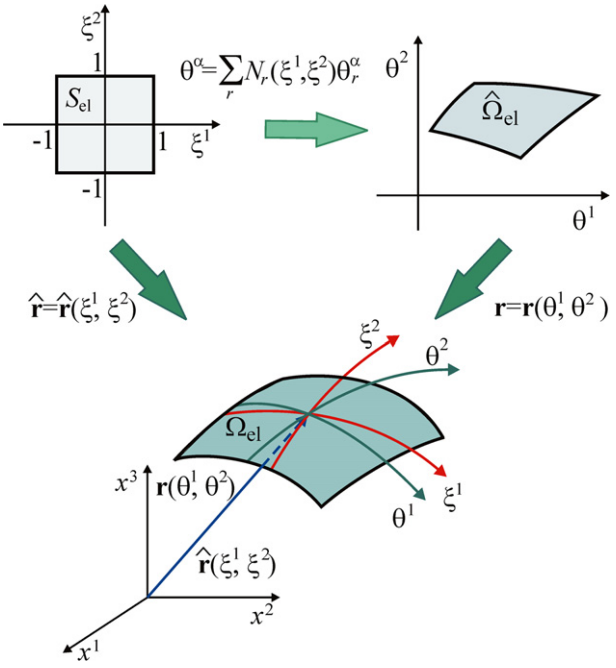

Fig. 5. Biunit square in (ξ^1, ξ^2)-space mapped into the geometrically exact shell element in (x^1, x^2, x^3)-space.

To realize the above, we write the principle of the virtual work (64), (72) and (73) for the shell element in matrix notations as follows:

$$\int\int_{S_{\rm el}} [\delta(\boldsymbol{\varepsilon}^I)^{\rm T}\mathbf{D}_{IJ}\boldsymbol{\varepsilon}^J - \delta\tilde{\mathbf{u}}^{\rm T}\mathbf{p}]\sqrt{a}\Lambda\,{\rm d}\xi^1\,{\rm d}\xi^2 - \delta W^{\Sigma}_{\rm ext} = 0, \tag{74}$$

where $S_{\rm el} = [-1,1]\times[-1,1]$ is the biunit square in (ξ^1,ξ^2)- space; Λ is the determinant of the transformation matrix; $\tilde{\mathbf{u}}$ is the displacement vector of the shell; $\boldsymbol{\varepsilon}^I$ are the strain vectors of I-surfaces; $\mathbf{p}$ is the surface traction vector; $\mathbf{D}_{IJ}$ are the constitutive stiffness matrices given by

$$\tilde{\mathbf{u}} = [u_1^1\ u_2^1\ u_3^1\ u_1^2\ u_2^2\ u_3^2\ u_1^3\ u_2^3\ u_3^3]^{\rm T}, \quad \boldsymbol{\varepsilon}^I = [\varepsilon^I_{11}\ \varepsilon^I_{22}\ \varepsilon^I_{33}\ 2\varepsilon^I_{12}\ 2\varepsilon^I_{13}\ 2\varepsilon^I_{23}]^{\rm T}, \tag{75}$$

$$\mathbf{p} = [-\mu^1 p_b^1 - \mu^1 p_b^2 - \mu^1 p_b^3\ 0\ 0\ 0\ \mu^3 p_t^1\ \mu^3 p_t^2\ \mu^3 p_t^3]^{\rm T},$$

$$\mathbf{D}_{IJ} = \int_{-d_b}^{d_t} \mu\mathbf{C}L_I^3 L_J^3\,{\rm d}\theta^3, \quad \Lambda = \det\left(\frac{\partial\theta^\beta}{\partial\xi^\alpha}\right), \tag{76}$$

where $\mathbf{C}$ is the elastic coefficients matrix defined as

$$\mathbf{C} = \begin{bmatrix} C^{1111} & C^{1122} & C^{1133} & C^{1112} & 0 & 0 \\ C^{2211} & C^{2222} & C^{2233} & C^{2212} & 0 & 0 \\ C^{3311} & C^{3322} & C^{3333} & C^{3312} & 0 & 0 \\ C^{1211} & C^{1222} & C^{1233} & C^{1212} & 0 & 0 \\ 0 & 0 & 0 & 0 & C^{1313} & C^{1323} \\ 0 & 0 & 0 & 0 & C^{2313} & C^{2323} \end{bmatrix}. \tag{77}$$

The finite element approximation of the displacement field can be written as

$$\tilde{\mathbf{u}} = \sum_r N_r\mathbf{u}_r \quad (r = 1,2,\ldots,NN), \tag{78}$$

where $N_r(\xi^1,\xi^2)$ are the shape functions of the element; NN is the number of nodes; $\mathbf{u}_r$ are the displacement vectors of element nodes given by

$$\mathbf{u}_r = [u_{1r}^1\ u_{2r}^1\ u_{3r}^1\ u_{1r}^2\ u_{2r}^2\ u_{3r}^2\ u_{1r}^3\ u_{2r}^3\ u_{3r}^3]^{\rm T}. \tag{79}$$

It is convenient further to introduce a displacement vector of the shell element of order $NDOF = 9\times NN$:

$$\mathbf{U} = [\mathbf{u}_1^{\rm T}\ \mathbf{u}_2^{\rm T}\ldots\mathbf{u}_{NN}^{\rm T}]^{\rm T}. \tag{80}$$

The use of this notation and approximation (78) into strain–displacement relationships (46) yields

$$\begin{aligned} \varepsilon^I_{11} &= \sum_p B^I_{1p}U_p + \sum_{p,q} A^I_{1pq}U_pU_q, \\ \varepsilon^I_{22} &= \sum_p B^I_{2p}U_p + \sum_{p,q} A^I_{2pq}U_pU_q, \\ &\ldots \\ 2\varepsilon^I_{23} &= \sum_p B^I_{6p}U_p + \sum_{p,q} A^I_{6pq}U_pU_q, \end{aligned} \tag{81}$$

where coefficients B^I_{sp} and A^I_{spq} depend on the shape functions and their derivatives and correspond to the linear and non-linear strain–displacement transformations. Throughout this section the index s runs from 1 to 6 and the indices p, q run from 1 to $NDOF$. Besides, a symmetry condition

$$A^I_{spq} = A^I_{sqp} \tag{82}$$

holds.

In a matrix form relations (81) can be represented in the following form (Kulikov and Plotnikova, 2007):

$$\boldsymbol{\varepsilon}^I = \mathbf{B}^I\mathbf{U} + (\mathbf{A}^I\mathbf{U})\mathbf{U} = (\mathbf{B}^I + \mathbf{A}^I\mathbf{U})\mathbf{U}, \tag{83}$$

where $\mathbf{B}^I$ are the matrices of order $6 \times NDOF$; $\mathbf{A}^I$ are the 3D arrays of order $6 \times NDOF \times NDOF$; $\mathbf{A}^I\mathbf{U}$ are the matrices of order $6 \times NDOF$ such that their elements are defined as

$$(\mathbf{A}^I\mathbf{U})_{sp} = \sum_q A^I_{spq}U_q. \tag{84}$$

Due to symmetry of the 3D arrays (82), we have

$$\delta\boldsymbol{\varepsilon}^I = (\mathbf{B}^I + 2\mathbf{A}^I\mathbf{U})\delta\mathbf{U}. \tag{85}$$

Introducing Eqs. (78), (83) and (85) into variational equation (74), one obtains element equilibrium equations

$$\mathbf{K}_S(\mathbf{U})\mathbf{U} = \mathbf{F}, \tag{86}$$

where $\mathbf{F}$ is the force vector and $\mathbf{K}_S(\mathbf{U})$ is the secant stiffness matrix given by

$$\mathbf{K}_S(\mathbf{U}) = \int\int_{S_{el}} (\mathbf{B}^I + 2\mathbf{A}^I\mathbf{U})^T\mathbf{D}_{IJ}(\mathbf{B}^J + \mathbf{A}^J\mathbf{U})\sqrt{a}\Lambda\, d\xi^1\, d\xi^2. \tag{87}$$

It is remarkable that the stiffness matrix (87) has been written in a very compact form, which is straightforward for the finite element implementation. Due to the fact that all non-linear terms have been retained in strain–displacement relationships (81), equilibrium equations (86) are highly non-linear algebraic equations. Future developments will be devoted to the approximate solution of these equations by the Newton–Raphson method. To realize the above, the symmetric tangent stiffness matrix $\mathbf{K}_T$ should be consistently derived. A short discussion on that is presented in Appendix C. Thus, the systems of linearized algebraic equations at each iteration and load step can be solved efficiently.

8. Conclusions

A compact and convenient finite deformation higher-order shell formulation has been presented in this work. This formulation is based on the use of displacements of *I*-surfaces inside the shell body as fundamental unknowns. In the case of choosing three, four and five equally located surfaces as *I*-surfaces, respectively 9, 12 and 15-parameter shell models have been developed. Such choice of unknowns allowed us to derive non-linear strain–displacement relationships, which exactly represent arbitrarily large rigid-body motions in a convected curvilinear coordinate system. All three finite deformation higher-order shell models take into account the non-linear distribution of the transverse normal strain through the shell thickness and, therefore, the 3D constitutive equations are utilized.

A weak form of equilibrium equations for the tensor-based 9-parameter shell formulation has been derived. It is noteworthy that the stiffness matrix has a very compact form that can be used efficiently for development of geometrically exact shell elements undergoing finite displacements and rotations.

The future and ongoing works will present the finite element implementation of the proposed theories. In particular, the use of *I*-surfaces could be extended to the analysis of laminate structures; the *I*-surfaces technique should be very convenient to develop so-called global–local approaches.

Appendix A. Derivatives of Lagrange polynomials

Herein, we represent the derivatives of Lagrange polynomials. Note that in accordance with a property of Lagrange polynomials (18), (22) and (26), namely,

$$\sum_I L^N_I = 1, \quad z \in [-d_b, d_t] \tag{A1}$$

the identity for derivatives

$$\sum_{I} L^{N}_{I,3} = 0, \quad z \in [-d_b, d_t] \tag{A2}$$

holds.

A.1. Lagrange polynomials of the second order

From Eq. (18) follows

$$\begin{aligned} L^{3}_{1,3} &= \frac{2}{h^2}(2z - z_2 - z_3), \\ L^{3}_{2,3} &= \frac{4}{h^2}(-2z + z_1 + z_3), \\ L^{3}_{3,3} &= \frac{2}{h^2}(2z - z_1 - z_2). \end{aligned} \tag{A3}$$

A.2. Lagrange polynomials of the third order

From Eq. (22) we find

$$\begin{aligned} L^{4}_{1,3} &= \frac{9}{2h^3}[-(z_3 - z)(z_4 - z) - (z_2 - z)(z_4 - z) - (z_2 - z)(z_3 - z)], \\ L^{4}_{2,3} &= \frac{27}{2h^3}[(z_3 - z)(z_4 - z) - (z - z_1)(z_4 - z) - (z - z_1)(z_3 - z)], \\ L^{4}_{3,3} &= \frac{27}{2h^3}[(z - z_2)(z_4 - z) + (z - z_1)(z_4 - z) - (z - z_1)(z - z_2)], \\ L^{4}_{4,3} &= \frac{9}{2h^3}[(z - z_2)(z - z_3) + (z - z_1)(z - z_3) + (z - z_1)(z - z_2)]. \end{aligned} \tag{A4}$$

A.3. Lagrange polynomials of the fourth order

From Eq. (26) one derives

$$\begin{aligned} L^{5}_{1,3} &= \frac{32}{3h^4}[-(z_3 - z)(z_4 - z)(z_5 - z) - (z_2 - z)(z_4 - z)(z_5 - z) \\ &\quad - (z_2 - z)(z_3 - z)(z_5 - z) - (z_2 - z)(z_3 - z)(z_4 - z)], \\ L^{5}_{2,3} &= \frac{128}{3h^4}[(z_3 - z)(z_4 - z)(z_5 - z) - (z - z_1)(z_4 - z)(z_5 - z) \\ &\quad - (z - z_1)(z_3 - z)(z_5 - z) - (z - z_1)(z_3 - z)(z_4 - z)], \\ L^{5}_{3,3} &= \frac{64}{h^4}[(z - z_2)(z_4 - z)(z_5 - z) + (z - z_1)(z_4 - z)(z_5 - z) \\ &\quad - (z - z_1)(z - z_2)(z_5 - z) - (z - z_1)(z - z_2)(z_4 - z)], \\ L^{5}_{4,3} &= \frac{128}{3h^4}[(z - z_2)(z - z_3)(z_5 - z) + (z - z_1)(z - z_3)(z_5 - z) \\ &\quad + (z - z_1)(z - z_2)(z_5 - z) - (z - z_1)(z - z_2)(z - z_3)], \\ L^{5}_{5,3} &= \frac{32}{3h^4}[(z - z_2)(z - z_3)(z - z_4) + (z - z_1)(z - z_3)(z - z_4) \\ &\quad + (z - z_1)(z - z_2)(z - z_4) + (z - z_1)(z - z_2)(z - z_3)]. \end{aligned} \tag{A5}$$

A.4. Verification

It can be verified that all polynomials (A3)–(A5) satisfy Eq. (A2) exactly.

Appendix B. Strain–displacement relationships in orthogonal curvilinear coordinate system

In the following, we briefly summarize the strain–displacement relationships for one particular case. If the reference surface Ω is referred to the orthogonal curvilinear coordinates, which coincide with the lines of principal curvatures of its surface, then

$$\begin{aligned} &\boldsymbol{a}_\alpha = A_\alpha \mathbf{e}_\alpha, \quad \boldsymbol{a}_3 = \mathbf{e}_3, \\ &b_1^1 = -k_1, \quad b_2^2 = -k_2, \quad b_1^2 = b_2^1 = 0, \end{aligned} \tag{B1}$$

where $\mathbf{e}_i$ are the orthonormal base vectors of the reference surface; A_α and k_α are the coefficients of the first fundamental form and principal curvatures of the reference surface. The use of Eq. (B1) in Eqs. (10) and (11) leads to

$$\mu_1^{I1} = c_1^I = 1 + k_1 z_I, \quad \mu_2^{I2} = c_2^I = 1 + k_2 z_I, \quad \mu_1^{I2} = \mu_2^{I1} = 0, \tag{B2}$$

$$\mathbf{g}_\alpha^I = A_\alpha c_\alpha^I \mathbf{e}_\alpha, \quad \mathbf{g}_3^I = \mathbf{e}_3. \tag{B3}$$

From Eqs. (39) and (B3) follow the needed strain–displacement relationships

$$\begin{aligned} 2\overset{\circ}{\varepsilon}{}^I_{\alpha\beta} &= \frac{1}{A_\alpha} c_\beta^I \mathbf{u}^I_{,\alpha} \cdot \mathbf{e}_\beta + \frac{1}{A_\beta} c_\alpha^I \mathbf{u}^I_{,\beta} \cdot \mathbf{e}_\alpha + \frac{1}{A_\alpha A_\beta} \mathbf{u}^I_{,\alpha} \cdot \mathbf{u}^I_{,\beta}, \\ 2\overset{\circ}{\varepsilon}{}^I_{\alpha 3} &= c_\alpha^I \boldsymbol{\beta}^I \cdot \mathbf{e}_\alpha + \frac{1}{A_\alpha} \mathbf{u}^I_{,\alpha} \cdot (\mathbf{e}_3 + \boldsymbol{\beta}^I), \\ 2\overset{\circ}{\varepsilon}{}^I_{33} &= \boldsymbol{\beta}^I \cdot (2\mathbf{e}_3 + \boldsymbol{\beta}^I), \end{aligned} \tag{B4}$$

where $\overset{\circ}{\varepsilon}{}^I_{ij}$ are the components of the Green–Lagrange strain tensor at the I-surfaces in the orthonormal reference surface frame.

The displacement vectors and transverse rate vectors of I-surfaces can be represented in this orthonormal frame as follows:

$$\mathbf{u}^I = \sum_i \overset{\circ}{u}{}_i^I \mathbf{e}_i, \tag{B5}$$

$$\boldsymbol{\beta}^I = \sum_i \overset{\circ}{\beta}{}_i^I \mathbf{e}_i. \tag{B6}$$

Taking into account Eq. (B5) and well-known formulas for the derivatives of unit vectors $\mathbf{e}_i$ with respect to orthogonal coordinates (see e.g. Kulikov and Plotnikova, 2007)

$$\begin{aligned} &\frac{1}{A_\alpha}\mathbf{e}_{\alpha,\alpha} = -B_{\alpha\beta}\mathbf{e}_\beta - k_\alpha \mathbf{e}_3, \quad \frac{1}{A_\alpha}\mathbf{e}_{\beta,\alpha} = B_{\alpha\beta}\mathbf{e}_\alpha \qquad \text{for } \beta \neq \alpha, \\ &\frac{1}{A_\alpha}\mathbf{e}_{3,\alpha} = k_\alpha \mathbf{e}_\alpha, \quad B_{\alpha\beta} = \frac{1}{A_\alpha A_\beta} A_{\alpha,\beta} \qquad \text{for } \beta \neq \alpha, \end{aligned} \tag{B7}$$

one derives

$$\frac{1}{A_\alpha}\mathbf{u}^I_{,\alpha} = \sum_i \lambda^I_{i\alpha} \mathbf{e}_i, \tag{B8}$$

where

$$\begin{aligned}
\lambda^I_{\alpha\alpha} &= \frac{1}{A_\alpha}\overset{\circ}{u}{}^I_{\alpha,\alpha} + B_{\alpha\beta}\overset{\circ}{u}{}^I_\beta + k_\alpha \overset{\circ}{u}{}^I_3 \quad \text{for } \beta \neq \alpha,\\
\lambda^I_{\beta\alpha} &= \frac{1}{A_\alpha}\overset{\circ}{u}{}^I_{\beta,\alpha} - B_{\alpha\beta}\overset{\circ}{u}{}^I_\alpha \quad \text{for } \beta \neq \alpha,\\
\lambda^I_{3\alpha} &= \frac{1}{A_\alpha}\overset{\circ}{u}{}^I_{3,\alpha} - k_\alpha \overset{\circ}{u}{}^I_\alpha.
\end{aligned} \tag{B9}$$

Substituting Eqs. (B6) and (B8) into Eq. (B4), we arrive at the final strain–displacement relationships

$$\begin{aligned}
2\overset{\circ}{\varepsilon}{}^I_{\alpha\beta} &= c^I_\alpha \lambda^I_{\alpha\beta} + c^I_\beta \lambda^I_{\beta\alpha} + \sum_i \lambda^I_{i\alpha}\lambda^I_{i\beta},\\
2\overset{\circ}{\varepsilon}{}^I_{\alpha 3} &= c^I_\alpha \overset{\circ}{\beta}{}^I_\alpha + \lambda^I_{3\alpha} + \sum_i \overset{\circ}{\beta}{}^I_i \lambda^I_{i\alpha},\\
2\overset{\circ}{\varepsilon}{}^I_{33} &= 2\overset{\circ}{\beta}{}^I_3 + \sum_i \overset{\circ}{\beta}{}^I_i \overset{\circ}{\beta}{}^I_i.
\end{aligned} \tag{B10}$$

It is worth noting that strain–displacement relationships (B10) are also invariant under arbitrarily large rigid-body motions.

Appendix C. Derivation of tangent stiffness matrix

The *right* multiplication of a vector $\mathbf{U}$ of order $NDOF$ by a 3D array $\mathbf{A}^I$ of order $6 \times NDOF \times NDOF$ generates the matrix $\mathbf{A}^I\mathbf{U}$ of order $6 \times NDOF$ whose elements are described by Eq. (84), that is,

$$(\mathbf{A}^I\mathbf{U})_{sp} = \sum_q A^I_{spq}U_q = \sum_q A^I_{sqp}U_q, \tag{C1}$$

since a symmetry condition (82) holds. As we remember, the index s runs from 1 to 6, whereas the indices p, q run from 1 to NDOF.

We can also define the *left* multiplication of any vector $\mathbf{W}$ of order 6 by a 3D array $\mathbf{A}^I$ of order $6 \times NDOF \times NDOF$ following the rule:

$$(\mathbf{W}\mathbf{A}^I)_{pq} = \sum_s A^I_{spq}W_s = \sum_s A^I_{sqp}W_s = (\mathbf{W}\mathbf{A}^I)_{qp}. \tag{C2}$$

This implies that $\mathbf{W}\mathbf{A}^I$ is the *symmetric* matrix of order $NDOF \times NDOF$.

There is a noteworthy transformation (Kulikov and Plotnikova, 2007) connecting right and left vector multiplications:

$$(\mathbf{A}^I\mathbf{U})^{\mathrm{T}}\mathbf{W} = (\mathbf{W}\mathbf{A}^I)\mathbf{U}. \tag{C3}$$

The proof of this statement is trivial. Really, comparing the components of vectors in left and right parts of Eq. (C3)

$$\begin{aligned}
[(\mathbf{A}^I\mathbf{U})^{\mathrm{T}}\mathbf{W}]_p &= \sum_s (\mathbf{A}^I\mathbf{U})^{\mathrm{T}}_{ps}W_s = \sum_s \left(\sum_q A^I_{spq}U_q\right)W_s,\\
[(\mathbf{W}\mathbf{A}^I)\mathbf{U}]_p &= \sum_q (\mathbf{W}\mathbf{A}^I)_{pq}U_q = \sum_q \left(\sum_s A^I_{spq}W_s\right)U_q,
\end{aligned}$$

one can see that both vectors are the same.

Let the vector $\mathbf{U} + \Delta\mathbf{U}$ be the solution of non-linear equilibrium equations (86). The use of this vector in Eq. (86) yields

$$\mathbf{K}_{\mathrm{S}}(\mathbf{U} + \Delta\mathbf{U})(\mathbf{U} + \Delta\mathbf{U}) = \mathbf{F}. \tag{C4}$$

Considering the secant stiffness matrix $\mathbf{K}_S(\mathbf{U})$ from Eq. (87) and omitting higher-order terms into (C4), we derive linearized element equilibrium equations

$$\mathbf{K}_T\Delta\mathbf{U} = \mathbf{F} - \mathbf{K}_S(\mathbf{U})\mathbf{U}, \tag{C5}$$

where $\mathbf{K}_T$ is the tangent stiffness matrix defined as

$$\mathbf{K}_T = \int\int_{S_{el}} (\mathbf{B}^I + 2\mathbf{A}^I\mathbf{U})^T\mathbf{D}_{IJ}(\mathbf{B}^J + 2\mathbf{A}^J\mathbf{U})\sqrt{a}\Lambda\,d\xi^1\,d\xi^2 + 2\int\int_{S_{el}} [\mathbf{D}_{IJ}(\mathbf{B}^J + \mathbf{A}^J\mathbf{U})\mathbf{U}]\mathbf{A}^I\sqrt{a}\Lambda\,d\xi^1\,d\xi^2. \tag{C6}$$

It should be noted that the derivation of the second integral required using the transformation (C3) in the following form:

$$(\mathbf{A}^I\Delta\mathbf{U})^T\mathbf{W}_I = (\mathbf{W}_I\mathbf{A}^I)\Delta\mathbf{U}, \tag{C7}$$

where $\mathbf{W}_I$ are the vectors of order 6 given by

$$\mathbf{W}_I = \mathbf{D}_{IJ}(\mathbf{B}^J + \mathbf{A}^J\mathbf{U})\mathbf{U}. \tag{C8}$$

As expected, the tangent stiffness matrix $\mathbf{K}_T$ is symmetric because the matrix $\mathbf{W}_I\mathbf{A}^I$ in the second integral (C6) is symmetric. This is due to (C8) and the definition of the left multiplication of vectors by 3D arrays $\mathbf{A}^I$.

References

Arciniega, R.A., Reddy, J.N., 2007. Tensor-based finite element formulation for geometrically nonlinear analysis of shell structures. Computer Methods in Applied Mechanics and Engineering 196, 1048–1073.

Basar, Y., Itskov, M., Eckstein, A., 2000. Composite laminates: nonlinear interlaminar stress analysis by multi-layer shell elements. Computer Methods in Applied Mechanics and Engineering 185, 367–397.

Brank, B., 2005. Nonlinear shell models with seven kinematic parameters. Computer Methods in Applied Mechanics and Engineering 194, 2336–2362.

Brank, B., Korelc, J., Ibrahimbegović, A., 2002. Nonlinear shell problem formulation accounting for through-the-thickness stretching and its finite element implementation. Computers & Structures 80, 699–717.

Buchter, N., Ramm, E., Roehl, D., 1994. Three-dimensional extension of nonlinear shell formulation based on the enhanced assumed strain concept. International Journal for Numerical Methods in Engineering 37, 2551–2568.

Cantin, G., 1968. Strain displacement relationships for cylindrical shells. AIAA Journal 6, 1787–1788.

Carrera, E., 2002. Theories and finite elements for multilayered, anisotropic, composite plates and shells. Archives of Computational Methods in Engineering 9, 1–60.

Carrera, E., 2003. Theories and finite elements for multilayered plates and shells: a unified compact formulation with numerical assessment and benchmarking. Archives of Computational Methods in Engineering 10, 215–296.

Carrera, E., Brischetto, S., 2007. Analysis of thickness locking in classical, refined and mixed multilayered plate theories. Composite Structures 82, 549–562.

Dawe, D.J., 1972. Rigid-body motions and strain–displacement equations of curved shell finite elements. International Journal of Mechanical Sciences 14, 569–578.

El-Abbasi, N., Meguid, S.A., 2000. A new shell element accounting for through-thickness deformation. Computer Methods in Applied Mechanics and Engineering 189, 841–862.

Kim, Y.H., Lee, S.W., 1988. A solid element formulation for large deflection analysis of composite shell structures. Computers & Structures 30, 269–274.

Krätzig, W.B., Jun, D., 2003. On "best" shell models – from classical shells, degenerated and multi-layered concepts to 3D. Archive of Applied Mechanics 73, 1–25.

Kulikov, G.M., 2001. Analysis of initially stressed multilayered shells. International Journal of Solids and Structures 38, 4535–4555.

Kulikov, G.M., 2004. Strain–displacement relationships that exactly represent large rigid shell displacements. Mechanics of Solids 39, 105–113.

Kulikov, G.M., Plotnikova, S.V., 2003. Non-linear strain–displacement equations exactly representing large rigid-body motions. Part I. Timoshenko-Mindlin shell theory. Computer Methods in Applied Mechanics and Engineering 192, 851–875.

Kulikov, G.M., Plotnikova, S.V., 2006a. Geometrically exact assumed stress–strain multilayered solid-shell elements based on the 3D analytical integration. Computers & Structures 84, 1275–1287.

Kulikov, G.M., Plotnikova, S.V., 2006b. Non-linear strain–displacement equations exactly representing large rigid-body motions. Part II. Enhanced finite element technique. Computer Methods in Applied Mechanics and Engineering 195, 2209–2230.

Kulikov, G.M., Plotnikova, S.V., 2007. Non-linear geometrically exact assumed stress–strain four-node solid-shell element with high coarse-mesh accuracy. Finite Elements in Analysis and Design 43, 425–443.

Librescu, L., 1987. Refined geometrically nonlinear theories of anisotropic laminated shells. Quarterly of Applied Mathematics 45, 1–22.

Parisch, H., 1995. A continuum-based shell theory for non-linear applications. International Journal for Numerical Methods in Engineering 38, 1855–1883.

Park, H.C., Cho, C., Lee, S.W., 1995. An efficient assumed strain element model with six dof per node for geometrically nonlinear shells. International Journal for Numerical Methods in Engineering 38, 4101–4122.

Sansour, C., 1995. A theory and finite element formulation of shells at finite deformations involving thickness change: circumventing the use of a rotation tensor. Archive of Applied Mechanics 65, 194–216.

Sansour, C., Kollmann, F.G., 2000. Families of 4-node and 9-node finite elements for a finite deformation shell theory. An assessment of hybrid stress, hybrid strain and enhanced strain elements. Computational Mechanics 24, 435–447.

Schoop, H., 1986. Oberflächenorientierte Schalentheorien endlicher Verschiebungen. Ingenieur-Archiv 56, 427–437.

Sze, K.Y., 2002. Three-dimensional continuum finite element models for plate/shell analysis. Progress in Structural Engineering and Materials 4, 400–407.

Zienkievicz, O.C., Taylor, R.L., 2000. The Finite Element Method. Volume 1: The Basis, fifth ed. Butterworth Heinemann, Oxford.